Materials Science Forum
ISSN: 1662-9752, Vol. 1004, pp 355-360

Submitted: 2019-09-27
Revised: 2020-01-20
Accepted: 2020-02-07
Online: 2020-07-28

Near Infrared Photoluminescence of $N_CV_{Si}^-$ Centers in High-Purity Semi-Insulating 4H-SiC Irradiated with Energetic Charged Particles

Shin-ichiro Sato[1,2,a*], Takuma Narahara[1,3,b], Shinobu Onoda[1,c], Yuichi Yamazaki[1,d], Yasuto Hijikata[3,e], Brant C. Gibson[2,f], Andrew D. Greentree[2,g], and Takeshi Ohshima[1,h]

[1]National Institutes for Quantum and Radiological Science and Technology, 1233 Watanuki, Takasaki, Gunma, JAPAN

[2]ARC Center of Excellence for Nanoscale BioPhotonics, RMIT University, Melbourne, Australia

[3]Saitama University, 255 Shimo-ohkubo, Sakura-ku, Saitama, Saitama, JAPAN

[a]sato.shinichiro2@qst.go.jp, [b]t.narahara.808@ms.saitama-u.ac.jp, [c]onoda.shinobu@qst.go.jp, [d]yamazaki.yuichi@qst.go.jp, [e]yasuto@opt.ees.saitama-u.ac.jp, [f]brant.gibson@rmit.edu.au, [g]andrew.greentree@rmit.edu.au, [h]ohshima.takeshi@qst.go.jp

Keywords: Radiation induced defects, Point defects, Color centers, Near infrared photoluminescence, Ion beam.

Abstract. This paper reports optical propertites of negatively charged $N_CV_{Si}^-$ centers in silicon carbide (a nitrogen substituting for a carbon atom adjacent to a silicon vacancy) whose emission wavlength is 1100-1500 nm at room temperature. High-purity semi-insulating (HPSI) 4H-SiCs are implanted with high energy N ion beams and subsequently thermally annealed to form N_CV_{Si} centers. We investigated a wide range of N ion implantation dose using a micro ion beam implantation technique and observed the photoluminescence intensity from the SiC-NV centers. We show that under conditions of heavy implantation, the excitation laser power excites residual defects and their fluorescences intereferes with the emission from the $N_CV_{Si}^-$ centers. These results allow us to clarify the requirements to optically detect isolated single $N_CV_{Si}^-$ centers at lightly implanted conditions.

Introduction

Atomic-scale spin defects in wide-gap semiconductors have attracted considerable attention because of their potential for quantum technology applications such as quantum information processing, quantum sensing, and quantum metrology [1-4]. Silicon Carbide (SiC) is one of the most attractive host materials for these applications and it has been reported that silicon vacancies (V_{Si}^-) [5-7] and divacancies ($V_{Si}V_C^0$) [8, 9] could serve as controllable spin states with sharp zero-phonon lines (ZPLs). One of the great advantages of SiC is that the crystal growth and device fabrication technology are well developed and thus SiC-based electrically driven qubits are feasible.

Recently, $N_CV_{Si}^-$ centers in SiC, *i.e.* negatively-charged pairs of V_{Si} and nitrogen (N) atom on an adjacent C site, have been explored, as they are an optically active defect with an electronic structure strongly resembling that of NV centers in diamond, which are well known as one of the most outstanding solid-state qubits/quantum sensors [10]. The ZPL of $N_CV_{Si}^-$ between the $^3A_2$ ground state and the ^3E excited state is located at around 1200 nm, much longer than that of NV centers in diamond (638 nm). This optical property is advantageous for *in vivo* imaging and sensing (temperature, magnetic field, etc.), since the near-infrared (NIR) light can penetrate biological tissues such as skin and blood more efficiently than visible light [11]. However, optical detection of single $N_CV_{Si}^-$ centers, which is necessary to achieve quantum sensing/imaging using $N_CV_{Si}^-$ centers with atomic-scale resolution, has not been realized yet. One of the reasons is that $N_CV_{Si}^-$ centers have not been seen in any as grown SiC materials and their formation mechanism is less well understood than other defect centers in SiC. $N_CV_{Si}^-$ centers can be introduced by energetic particle irradiation (defect formation) and subsequent thermal annealing. For example, Bardeleben *et al.* have reported that $N_CV_{Si}^-$ centers were formed by 12 MeV proton irradiation at the fluence of 1×10^{16} cm^{-2} and subsequent thermal

annealing at 900 °C in n-type 4H-SiC [12]. In this irradiation condition, a large vacancy density was introduced in the material and hence formation of single $N_CV_{Si}^-$ centers would not be expected.

In Ref. [13], we have shown that arrays of ion-beam written ensembles are a great tool to characterize quantum color centers. Here we show the creation of arrays of ensembles of $N_CV_{Si}^-$ centers by nitrogen ion beam implantation to SiC. We investigate the NIR photoluminescence (PL) properties of 4H-SiCs implanted with energetic nitrogen ions for the purpose of clarifying the formation mechanism and for detecting the single $N_CV_{Si}^-$ centers. The dependences of implantation dose and excitation laser power density are clarified, as is the role of residual defects formed by the implantation process.

Experimental

The sample used in this study was High Purity Semi-Insulating (HPSI) 4H-SiC substrate with nitrogen (N) concentration of 3×10^{15} cm^{-3}. Little luminescence appeared at NIR regions (above 1100 nm) in the unirradiated HPSI-4H-SiCs. To create $N_CV_{Si}^-$ centers we irradiated this sample with 10 MeV N ions at room temperature. The ion implantation was performed at the Takasaki Advanced Radiation Research Institute, National Institutes for Quantum and Radiological Science and Technology. The 10 MeV N ions was focused on the sample surface to obtain micrometer-sized beam and only specific regions (spots) were irradiated. The average number of implanted N ions in each spot, which was determined from the average N ion beam flux and the irradiation time, was varied from 2 N/spot to 2×10^6 N/spot. The implantation pattern is schematically illustrated in Fig. 1. After implantation, the sample was thermally annealed at 1000 °C for 30 min under Ar atmosphere using an infrared heating furnace. It was revealed from our previous study that the optimal annealing temperature for the $N_CV_{Si}^-$ center formation was 1000 °C [14]. The average range of 10 MeV N ions was estimated to be 4.8 µm, according to the Monte Carlo Simulation Code, TRIM [15]. The lateral straggling and the radial straggling were also estimated to be 134 nm and 173 nm, respectively, being far smaller than the microbeam diameter. Thus, the location of created $N_CV_{Si}^-$ centers was dominated by the microbeam position and diameter.

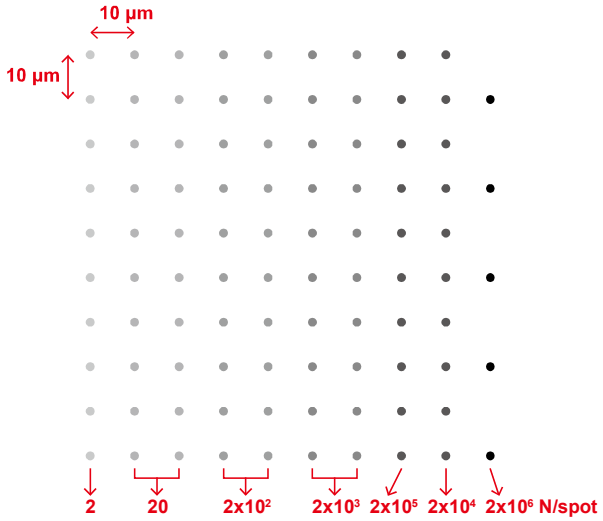

Fig. 1. Implantation pattern of 10 MeV N ions. The pitch of the array is 10 µm. The irradiated doses in each spot are shown in red.

Optical properties of the sample were investigated using a home-build confocal microscope (CFM). Fig. 2 shows the schematic drawing of CFM used in this study. Spectroscopy was performed with laser excitation wavelength at 980 nm and power densities at 1.3×10^2 kW/cm^2.

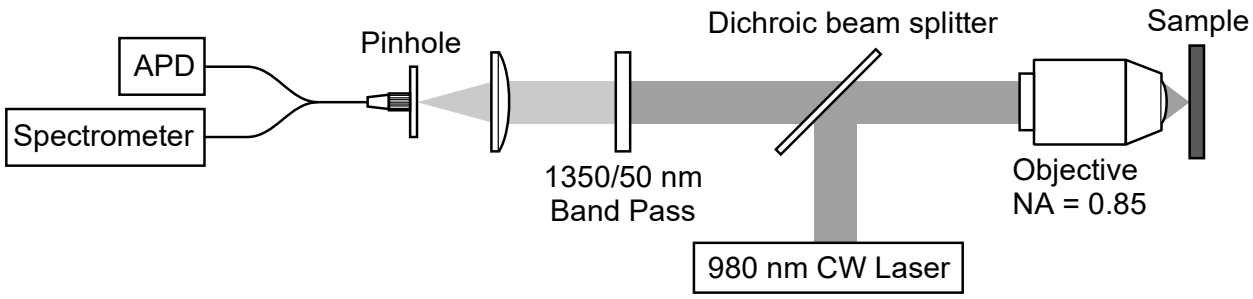

Fig. 2. Schematic drawing of CFM used in this study. The sample was excited with a 980 nm continuous wave laser, and the signal was either detected with an avalanche photo diode (APD) after a 1350 nm bandpass filter or directly analyzed with a spectrometer.

Photoluminescence from the implanted region was collected with an NIR objective lens (numerical aperture, NA = 0.85) and detected by an InGaAs avalanche photo-diode (APD). The expected laser spot diameter and lateral resolution of CFM used in this study were 1.4 μm and 0.59 μm, respectively. The PL spectra were investigated by an imaging spectrometer installed in the CFM. A 1350 nm band pass filter (50 nm band width) was placed in front of the APD to selectively collect photons emitted from $N_CV_{Si}^-$ centers. All measurements were performed at room temperature.

Results and Discussion

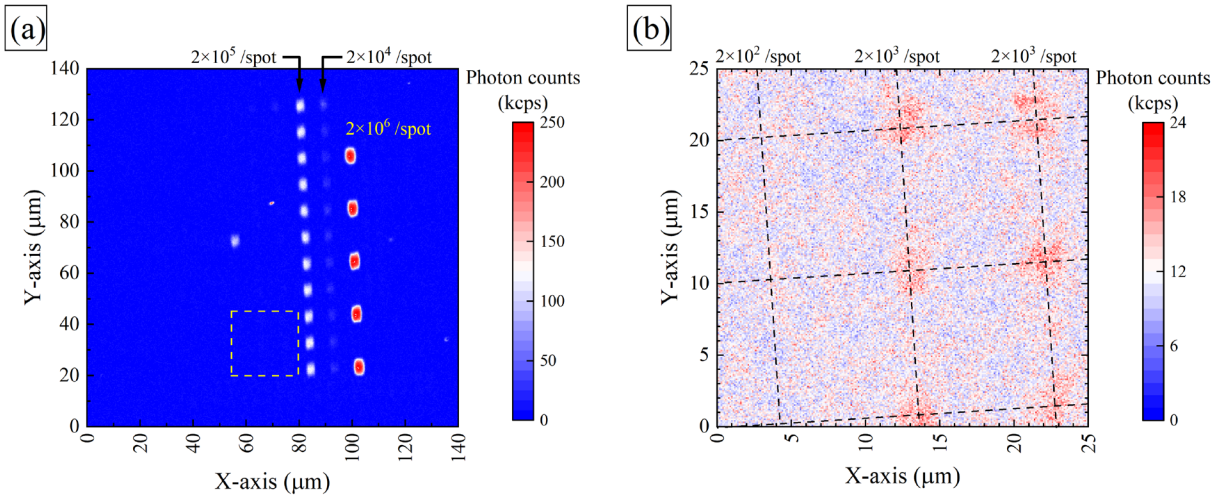

Fig. 3. CFM images of the irradiated regions of sample. (a) wide image, (b) fine image of the yellow dashed square region in (a). The excitation laser power was 1.3×10^2 kW/cm^2 in both images. A grid by dashed lines in (b) is drawn to indicate the irradiated regions. Note that due to the large variation in spot brightness, it is not possible to reliably resolve the spots with less than 2×10^4 N/spot in the wide scan, although regions with 2×10^3 N/spot were visible on the fine scan. Spots with 2×10^2 N/spot or less were not detectable above background.

CFM images of the whole implanted region is shown in Fig. 3 (a). Ten regions of 2×10^5 N/spot and 2×10^4 N/spot implantations, and 5 regions of 2×10^6 N/spot implantation were observed as indicated as arrows in the figure. The fluorescence counts increased with increasing implanted dose, which is presumably due to the increased number of centers formed. PL spectra of the irradiated regions of 2×10^6 N/spot, 2×10^5 N/spot, and 2×10^4 N/spot are shown in Fig. 4. A broad peak centered at 1260 nm appeared in all PL spectra. Since these PL spectra are identical to the PL spectrum of N_CV_{Si} centers at room temperature which has been reported previously [14], the CFM image in Fig. 3 (a) indicates the spatial distribution of N_CV_{Si} centers formed by 10 MeV N ion implantation and subsequent thermal annealing. Note that only the luminescence around 1350 nm (50 nm band), shown by dashed lines in Fig. 4., was collected using the band pass filter to obtain the CFM image in Fig. 2. Implanted regions with less than 2×10^4 N/spot were not clearly found in Fig. 3 (a). Fig. 3 (b) shows the fine CFM image in the region enclosed by a yellow dashed line in Fig. 3 (a). The 2×10^3 N/spot irradiated regions appeared as luminescent regions with 10 μm intervals, whereas no luminescent region was found from the 2×10^2 N/spot irradiated regions. In other words, the fluorescence counts at the 2×10^2 N/spot irradiated regions were almost comparable to that of backgrounds (BG) and the presence of color centers formed by 10 MeV N ion implantation and subsequent thermal annealing was not verified. The luminescent area of 2×10^4 N/spot irradiated region was estimated to be roughly 2×3 μm^2 and thus the implantation of 2×10^3 N/spot corresponded to the fluence of 3×10^{10} cm^{-2}. Our earlier studies showed that 3×10^{12} cm^{-2} was the minimum fluence of N ions required to observe PL from N_CV_{Si} centers in HPSI-4H-SiC [14]. Compared to the previous report, this study demonstrates a 100-fold improvement of the optical detection of $N_CV_{Si}^-$ centers. However, further improvement of optical

detection sensitivity and the signal to BG ratio is required to reliably detect isolated single $N_CV_{Si}^-$ centers. In particular, it is known that the luminescent intensity of $N_CV_{Si}^-$ centers strongly depends on the excitation wavelength [16] and hence the optimal excitation wavelength should be clarified by photoluminescence excitation measurement.

The fluorescence counts of observed irradiated regions as a function of number of irradiated N ions are shown in Fig. 5. Five implanted regions at 2×10^4 N/spot, 2×10^5 N/spot, and 2×10^6 N/spot, and 10 implanted regions at 2×10^3 N/spot were explored. The ordinate is the net fluorescence counts with the BG subtracted and the data with three different laser power densities are also shown. When focusing on the results of 26 kW/cm^2 (blue open triangles), the net fluorescence counts increased with increasing number of irradiated N ions, but the rate of increase was below 1. This fact indicates that the formation probability of $N_CV_{Si}^-$ centers decreased with increasing the number of irradiated N ions and/or the quenching/non-radiative recombination due to higher residual defects and other defect centers. In addition, no significant luminescence was found from the 2×10^3 N/spot irradiated region when the laser power density was below 1.3×10^2 kW/cm^2.

The net fluorescence counts from single spots in the 2×10^4 N/spot, 2×10^5 N/spot, and 2×10^6 N/spot implanted regions as a function of laser power density are shown in Fig. 6. The ordinate is the net fluorescence counts of implanted regions. The excitation power dependence (saturation behavior) of photon emission intensity of color centers can be generally expressed as:

$$I \propto \left(1 + \frac{W_0}{W}\right)^{-1} \quad (1)$$

where I, W, and W_0 are the fluorescence counts from luminescent centers, the laser power density, and the saturation power density, respectively [17]. The calculated results, shown as solid lines in Fig. 6, are well fitted to the experimental data, and we obtain W_0 = 556 kW/cm^2 for 2×10^4 N/spot, 268 kW/cm^2 for 2×10^5 N/spot, and 75.0 kW/cm^2 for 2×10^6 N/spot. The saturation power density decreased with increasing the number of irradiated N ions. This trend may indicate that residual vacanies and other defect centers also increase with increasing number of

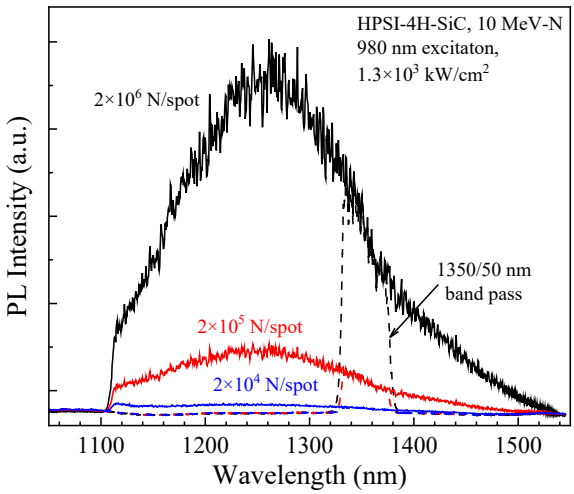

Fig. 4. PL spectra at the implanted regions: 2×10^6 N/spot (black), 2×10^5 N/spot (red), and 2×10^4 N/spot (blue). Solid and dashed lines are the spectra when 1100 nm long pass and 1350 nm band pass (50 nm band) filters were used, respectively.

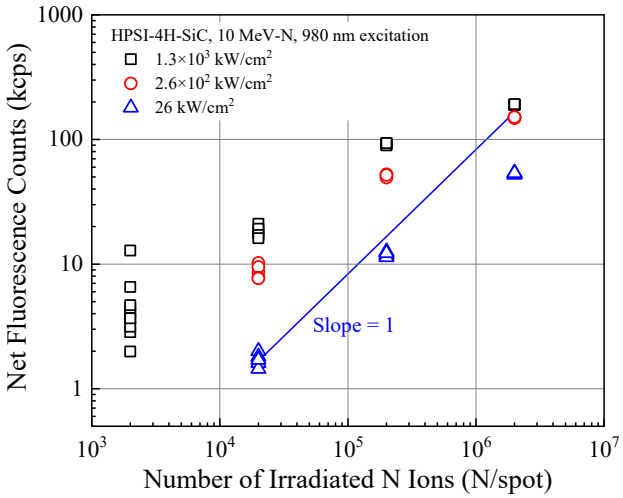

Fig. 5. Observed fluorescence counts of the implanted regions as a function of number of implanted N ions per spot. Black squares, red circles, and blue triangels denote the results of laser power densities of 1.3×10^3 kW/cm^2, 2.6×10^2 kW/cm^2, and 26 kW/cm^2 respectively. A linear line (slope = 1) is drawn to guide the eye. The net fluorescent counts grew slower than linear. The variability at the 2×10^3 N/spot is presumably due to Poisson statistics for the N_CV_{Si} center formation.

irradiated N ions and interfere the excitation and/or relaxation (luminescent transition) of $N_CV_{Si}^-$ centers.

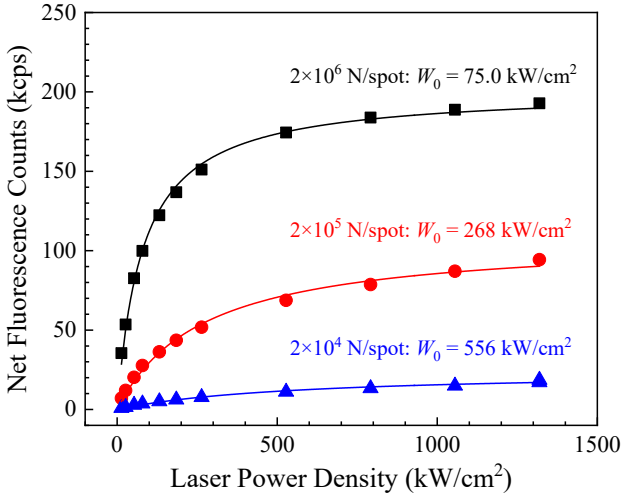

Fig. 6. Fluorescence counts of the implanted regions as a function of laser power density. Black squares, red circles, and blue triangles denote the data of 2×10^6 N/spot, 2×10^5 N/spot, and 2×10^4 N/spot, respectively. Solid lines are fitting curves by Eq. (1).

Summary

We reported PL properties of $N_CV_{Si}^-$ centers formed in the HPSI-4H-SiC by 10 MeV N ion implantation and subsequent thermal annealing at 1000 °C. To enable a systematic study of implantation conditions, we used a microbeam implantation technique over a wide range of dose and a NIR confocal microscope. The dependence of number of implanted N ions showed that the $N_CV_{Si}^-$ center formation appeared at above 2×10^3 N/spot, which is 100 times lower than the previously reported dose to create $N_CV_{Si}^-$ centers. Nevertheless, we were unable to identify isolated single $N_CV_{Si}^-$ centers, and further optimization in terms of the excitation wavelength and optical detection sensitivity are required before isolated single $N_CV_{Si}^-$ centers can be observed. The net photon emission from the implanted regions grew slower than linear with both implant dose and excitation intensity. This leads us to conclude that there are significant interactions with other defect centers. This could be due to either or both of a decreased center formation efficiency with dose, and quenching or other non-radiative interactions between the $N_CV_{Si}^-$ centers and other defect centers in the lattice. Further experiments are required to evaluate these different alternatives, and the measurement of implanted isolated single $N_CV_{Si}^-$ centers will greatly assist in resolving the issue.

Acknowledgement

This study was supported by the JSPS KAKENHI Grant Numbers 17H01056 and 18H03770, and the Australian Research Council, Grant Numbers CE140100003, LE140100131 and FT160100357. A part of this study was carried out within the framework of QST international research initiative “Quantum biosensors in wide-bandgap semiconductors”.

References

[1] J.R. Weber, W.F. Koehl, J.B. Varley, A. Janotti, B.B. Buckley, C.G. Van de Walle, D.D. Awschalom, Proc. Natl. Acad. Sci. U.S.A. 107 (2010) 8513-8518.

[2] T. Wolf, P. Neumann, K. Nakamura, H. Sumiya, T. Ohshima, J. Isoya, J. Wrachtrup, Phys. Rev. X 5 (2015) 041001.

[3] V.M. Acosta, E. Bauch, M.P. Ledbetter, C. Santori, K.M.C. Fu, P.E. Barclay, R.G. Beausoleil, H. Linget, J.F. Roch, F. Treussart, S. Chemerisov, W. Gawlik, D. Budker, Phys. Rev. B 80 (2009) 115202.

[4] T. Ohshima, T. Satoh, H. Kraus, G.V. Astakhov, V. Dyakonov, P.G. Baranov, Journal of Physics D: Applied Physics 51 (2018) 333002.

[5] S.A. Tarasenko, A.V. Poshakinskiy, D. Simin, V.A. Soltamov, E.N. Mokhov, P.G. Baranov, V. Dyakonov, G.V. Astakhov, Phys. Status Solidi B 255 (2018) 1700258.

[6] Y. Yamazaki, Y. Chiba, T. Makino, S.-I. Sato, N. Yamada, T. Satoh, Y. Hijikata, K. Kojima, S.-Y. Lee, T. Ohshima, J. Mater. Res. 33 (2018) 3355-3361.

[7] Y. Chiba, Y. Yamazaki, T. Makino, S. Sato, N. Yamada, T. Satoh, K. Kojima, S.Y. Lee, Y. Hijikata, T. Ohshima, Materials Science Forum 963 (2019) 709-713.

[8] D.J. Christle, A.L. Falk, P. Andrich, P.V. Klimov, J.U. Hassan, N.T. Son, E. Janzen, T. Ohshima, D.D. Awschalom, Nat. Mater. 14 (2015) 160-163.

[9] C.F. de las Casas, D.J. Christle, J. Ul Hassan, T. Ohshima, N.T. Son, D.D. Awschalom, Appl. Phys. Lett. 111 (2017) 262403.

[10] J. Wrachtrup, F. Jelezko, J. Phys. Condens. Mat. 18 (2006) S807-S824.

[11] A.M. Smith, M.C. Mancini, S. Nie, Nat. Nanotechnol. 4 (2009) 710-711.

[12] H.J. von Bardeleben, J.L. Cantin, E. Rauls, U. Gerstmann, Phys. Rev. B 92 (2015) 064104.

[13] H. Kraus, D. Simin, C. Kasper, Y. Suda, S. Kawabata, W. Kada, T. Honda, Y. Hijikata, T. Ohshima, V. Dyakonov, G.V. Astakhov, Nano Lett. 17 (2017) 2865-2870.

[14] S.-i. Sato, T. Narahara, Y. Abe, Y. Hijikata, T. Umeda, T. Ohshima, J. Appl. Phys. 126 (2019) 083105.

[15] J.F. Ziegler, M.D. Ziegler, J.P. Biersack, Nucl. Instr. Meth. B 268 (2010) 1818-1823.

[16] B. Magnusson, N.T. Son, A. Csóré, A. Gällström, T. Ohshima, A. Gali, I.G. Ivanov, Phys. Rev. B 98 (2018) 195202.

[17] F. Fuchs, B. Stender, M. Trupke, D. Simin, J. Pflaum, V. Dyakonov, G.V. Astakhov, Nat. Commnun. 6 (2015) 7578.